

degradation in ferromagnetic structural steels. A better nondestructive measurement setup could be needed in actual application.

References

- [1] Ara K., Ebine N. and Nakajima N., *J. Pressure Vessel Tech., Trans. ASME*, vol. 118, pp. 447-453 (1996)
- [2] K.Popp, M.Blochwitz, G.Brauer, E.Hampe, W.D.Leonhardt, and H.P.Schützler: *Kernenergie*, vol. 29, pp. 22-24 (1986)
- [3] N. Ebine and K. Ara, *Tech. Meeting of Mag. Soc., IEEE Japan*, paper No. MAG-98-198, 1998. (in Japanese)
- [4] Noriya Ebine and Katsuyuki Ara, *Magnetical Measurement To Evaluate Material Properties Of Ferromagnetic Structural Steels With Planar Coils*, *IEEE Transactions on Magnetics*, Vol.35 No.5 pp.3928-3930 (1999)
- [5] N.Ebine et al, *Correlation between the Magnetic and Mechanical Properties of Ferromagnetic Structural Steels, A533B and SUS410*, *J. Magnetic Soc. Japan*, Vol.20, No.2, pp.665-668, 1996

Reconstruction of Magnetization from Magnetic Flux Leakage for Evaluation of Material Degradation

Shigeru Takaya, Gabriel Preda, Kazuyuki Demachi, Tetsuya Uchimoto and Kenzo Miya
School of Engineering, University of Tokyo
Tokai-mura Naka-gun Ibaraki 319-1106, Japan

Abstract. Inverse analysis of the magnetization and the susceptibility distribution in stainless steel is proposed in this paper as a future technique to diagnose degradation before the outbreak of cracks. Neural Networks (NN) and regularization methods such as Principal Component Analysis, Shifting Aperture are proposed to cope with the ill posedness of the problem. A sample with cracks was obtained by exposing the specimen to a cyclic test. The magnetic flux density of the sample was then measured. A reconstruction of magnetization distribution is then obtained by inverse analysis. The accuracy of this method is confirmed by comparison between magnetic flux density due to reconstructed magnetization and measured results. Furthermore, the susceptibility is reconstructed for simulated data.

1. Introduction

Some non-magnetic structural steels used in power plants show presence of passive magnetic flux leakage at the stress concentration parts [1][2]. This is supposed to be due to the martensitic phase transformation inside the material during the loading cycles. Therefore, it is possible to estimate the material degradation by inverse analysis of magnetization or martensitic phase distribution from magnetic flux density scanned outside the steel [3]. The advantage of this new method compared with the usual methods is that the degradation can be evaluated by NDT before the outbreak of cracks. In this study, the magnetization distribution in a sample with cracks obtained by a cyclic test is reconstructed by using measurement magnetic flux density. Furthermore, reconstruction of magnetic susceptibility is proposed because there is some relationship between the rate of the martensitic transformation and the magnetic susceptibility χ [4]. The martensitic phase distribution in a plate magnetized by a uniform external magnetic field is taken into account. A method based on NN for reconstructing the magnetization and the susceptibility distribution from the magnetic flux density is developed.

2. Forward Analysis

In this study, a neural network is used for reconstructing the magnetization and

magnetic susceptibility distribution inside a specimen from the magnetic flux density distribution measured outside the specimen. Usually, neural networks need a lot of input data sets (the magnetic flux density, in this case) and output data (magnetization or susceptibility distribution) for training. That data is simulated numerically because it is very difficult to obtain large enough data sets from experiments.

The procedure of making training sets for reconstructing magnetization is as follows; at first, a certain magnetization distribution is assumed, then the magnetic flux density is calculated by using Biot-Savart law.

$$\mathbf{B}_i = \frac{\mu_0}{4\pi} \int_{\Omega} \frac{(\nabla \times \mathbf{M}_j) \times \mathbf{r}}{r^3} dV + \frac{\mu_0}{4\pi} \oint_{\partial\Omega} \frac{(\mathbf{M}_j \times \mathbf{n}) \times \mathbf{r}}{r^3} dS \quad \mathbf{r} = \mathbf{r}_s - \mathbf{r}_f \quad i = 1..n_s \quad (1)$$

where \mathbf{B}_i is the magnetic flux density due to the magnetization in the material at the measurement point i , \mathbf{M}_j is the magnetization of j -th element of a sample divided into n_s elements, \mathbf{n} is a normal vector on the surface, \mathbf{r}_s and \mathbf{r}_f are position vectors of source and field (measurement) points respectively. In this case, the first term of right hand is taken into account.

The simulation code making training sets for reconstructing magnetic susceptibility is based on FEM-BEM coupling based on A-formulation [5]. The overall procedure implies the following steps:

- 1) A certain susceptibility distribution is assumed. (In this study, the linear relation between magnetic field and magnetization is assumed because the magnetic field is small enough.); We solve the forward problem consisting of computation of the field inside the material due to the excitation by external magnetic field;
- 2) From the magnetic field distribution inside the material, the value of magnetization inside the material is deduced; the magnetic field outside the material is computed using Biot-Savart law (both terms of (1) is taken into account.);
- 3) Finally, using the previously computed data-set from several simulations with different susceptibility distributions, the NN is trained and reconstruction is performed.

3. Neural Network principle

An auto-adaptive feed-forward Neural Network (NN) is used to reconstruct the magnetization and magnetic susceptibility distribution from the leakage magnetic flux density distribution (Fig.1). The two main characteristics of this NN are as follows. First, input nodes are connected directly to not only the hidden nodes but also the output nodes. The additional connections between inputs and outputs account for the mapping linearities. Second, the training starts with only one hidden node, and for each training epoch a new node is created. In this way, the best network configuration both for learning and generalization is achieved through a dynamical adaptation of the NN configuration.

The new input-hidden connections receive random weights when they are created. The input-output and hidden-output interconnection weights, \mathbf{W}_{io} , \mathbf{W}_{ho} are obtained as least square error solution of the next over-determined system equation:

$$\left[\mathbf{X}^i, f_1(\mathbf{X}^i \cdot \mathbf{W}_{ih}) \right] \cdot \begin{bmatrix} \mathbf{W}_{io} \\ \mathbf{W}_{ho} \end{bmatrix} = f_2^{-1}(\mathbf{Y}^i), \quad (2)$$

where \mathbf{X}^i and \mathbf{Y}^i represent the input and output training sets matrices respectively, f_1 and f_2 are

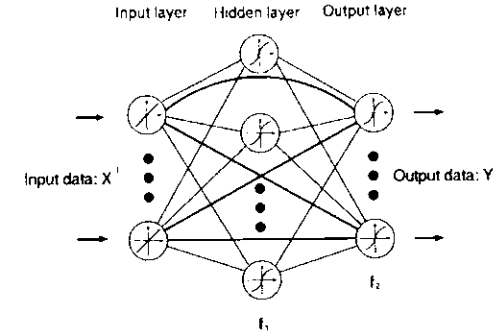


Fig. 1 Neural network architecture

the nonlinear activation functions applied to the hidden and output nodes. For every training step, after the weights are determined, the verification sets are propagated through the NN. The verification error is then evaluated and the weights values corresponding to optimum configuration in terms of reconstruction error are stored for usage in actual reconstruction. For this problem, Input data are magnetic flux density values and Output data are magnetization or magnetic susceptibility distribution values.

NN training is highly time and memory consuming because of its structure complexity when the number of input and output nodes is too large. In this study, NN performance is enhanced by Principal Component Analysis (PCA) and a 2 dimensional Shifting Aperture method [6]. PCA allows dimension reduction by projecting the data on the principal variation directions and keeping only the most significant directions' components. The multicollinearities of the data set are also eliminated. Shifting Aperture is basically a data-fragmentation and data-fusion method and was proved to be effective as an additional regularization method [6]. It is important to note that, after training, the network can reconstruct magnetization and susceptibility distribution regardless of the reconstructing area because its result is obtained as a weighted superposition of each aperture's result.

4. Reconstruction of magnetization distribution around cracks

The shape of the sample (SUS304) is shown in Fig. 2. There is a slit (3 mm×0.3 mm) at the center of the sample. Cracks (~3mm) appeared at the ends of the slit as a result of a cyclic test (range: 0.5% loading speed: 0.1%/sec). The sample was also pre-stressed subjecting it to a tensile test. The loading direction was y direction.

Figure 3 shows the y and z components of measured magnetic flux density. The shape of the sample is shown, too. The range of measurement is 3 mm × 3 mm, measured pitch is 1 mm and lift off is 0.5 mm. The measured result shows large values around cracks and a strong relation between a crack and magnetic flux density is recognized. From these results, three components of the magnetization distribution are reconstructed. The distribution of the absolute value and x, y components of magnetization is shown in Fig.4, 5. The magnetization shows large values around cracks.

The magnetic flux density is calculated by using (1) to verify the accuracy of reconstructed magnetization distribution (Fig.6). Comparison on $y = 2$ mm is shown in Fig. 7. It is confirmed that the magnetic flux density due to reconstructed magnetization and measured data agree well.

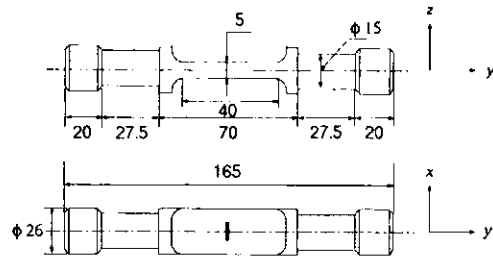


Fig.2 the shape of sample

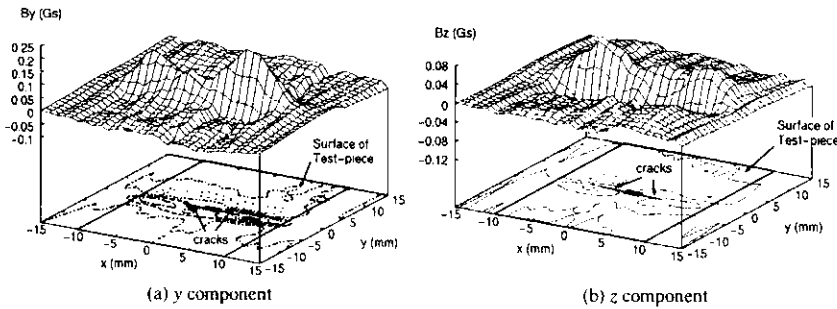


Fig.3 measurement magnetic flux density

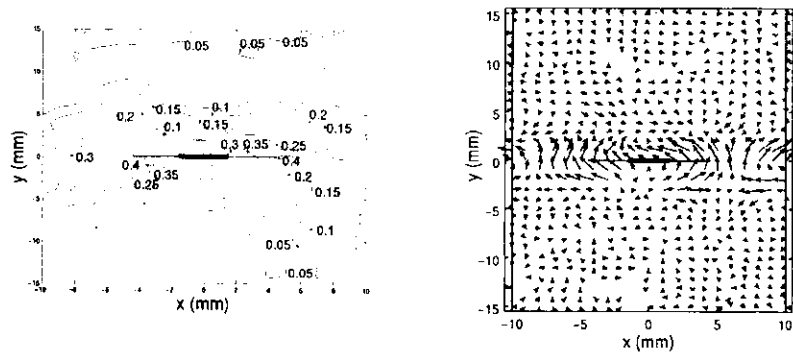


Fig.4 the absolute value of magnetization Fig.5 vector expression of x, y components of magnetization

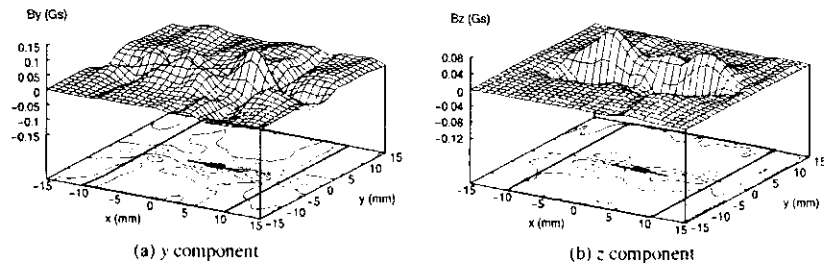


Fig.6 magnetic flux density due to reconstructed magnetization

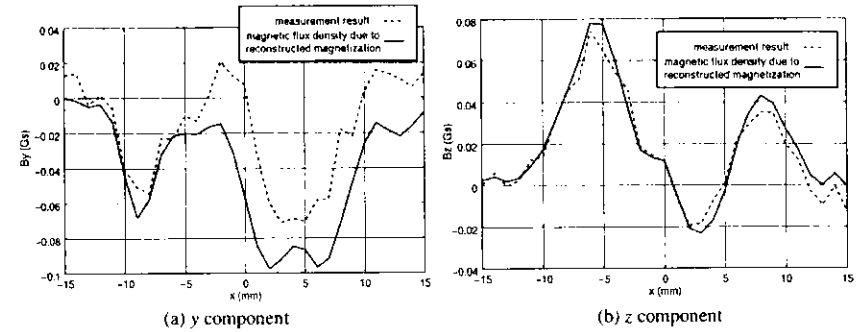


Fig.7 Comparison between measured magnetic flux density and one calculated using reconstructed magnetization distribution.

5. Reconstruction of magnetic susceptibility

The magnetization distribution was reconstructed by using measurement data of magnetic flux density. But in this case, martensitic phase is magnetized by natural magnetization or due to external environment, so we can estimate only the region of material degradation.

It is found experimentally that susceptibility has some relationship with the rate of martensitic transformation[4]. In this study, it is also proposed to reconstruct susceptibility from magnetic flux density due to magnetization by the external magnetic field.

5.1 Training data

The shape of a sample proposed in training sets is 10x10 mm length and 3 mm thick. The specimen is divided into 10x10 elements in xy plane and 3 elements in z direction. The scan region of magnetic flux density is the same 10x10 length as a sample. Liftoff is 0.5 mm and pitch, is 1 mm. It is assumed that magnetization is distributed in one cylinder having radius R; values of R are set 2, 3 or 4 mm randomly for the training set (Fig.8). In that cylinder, the susceptibility has distribution following a next equation in xy plane,

$$\chi(x, y) = \chi(x_c, y_c) \exp\left(-\frac{(x-x_c)^2 + (y-y_c)^2}{R^2}\right), \quad (3)$$

where (x_c, y_c) is the center of the circle and $\chi(x_c, y_c)$ is given randomly within range from 0 to 1000 each layer. In some case, there are layers where the susceptibility is zero in the whole region. The layers with martensitic phase continue and their values change monotonously in z direction. The external magnetic field is uniform spatially and its value is 500 Gauss only in z direction. 300 sets for training and 100 sets for validation are made.

5.2 The structure of neural network

In this study, shifting aperture method is used. An aperture contains the magnetic susceptibility values of $5 \times 5 \times 3$ (x, y, z direction, respectively) elements and x, y, and z components of magnetic flux density due to magnetization at 6×6 measurement points, which is compressed to 20 by PCA. The number of input nodes is 20 and that of output nodes

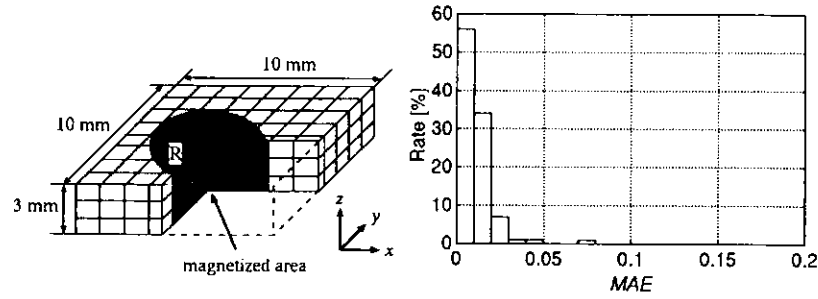


Fig. 8 a sample of training sets

Fig. 9 error distribution about verification sets

is 75 because the input is magnetic flux density and the output is susceptibility distribution in this case.

5.3 Error distribution for verification sets

The error distribution of verification sets (100 cases) is shown in Fig. 9 after training the NN with simulated data. The number of hidden nodes is 706. The horizontal axis is mean absolute error per lattice points (*MAE*) and the vertical axis is its ratio. *MAE* is calculated using (4).

$$MAE = \sum_{i=1}^N |\chi_{t,i} - \chi_{r,i}| / N, \tag{4}$$

where $\chi_{t,i}$, $\chi_{r,i}$ are susceptibility of the training data and the reconstructed result at element i respectively and N is the number of elements. The average of *MAE* is 0.012. The results show good quality of reconstruction.

For example, one case of reconstructed results of susceptibility distribution for the verification sets is shown in Fig. 10, 11. Figure 10, (a) shows a contour of true susceptibility distribution, (b) shows the reconstructed susceptibility distribution, and Fig. 11 shows the difference between true and reconstructed results on $x = 6$ mm. From those results, reasonable reconstruction is confirmed.

6. Conclusion

A method for reconstructing magnetization using Neural Network was developed. Furthermore, the magnetization distribution of a sample with a crack was reconstructed by this method. The presence of magnetization around the crack is confirmed from reconstructed magnetization. The magnetic flux density due to reconstructed magnetization and measured data are compared to verify the quality of the reconstructed magnetization, and these values agree well. A method for reconstructing susceptibility under uniform magnetic field is also developed. Reconstructed results show agreement with true distributions for simulation data. The susceptibility seems to have relation to the rate of martensitic transformation. From our first results, we can estimate that this method will allow us to evaluate the degree of material degradation more precisely in the future.

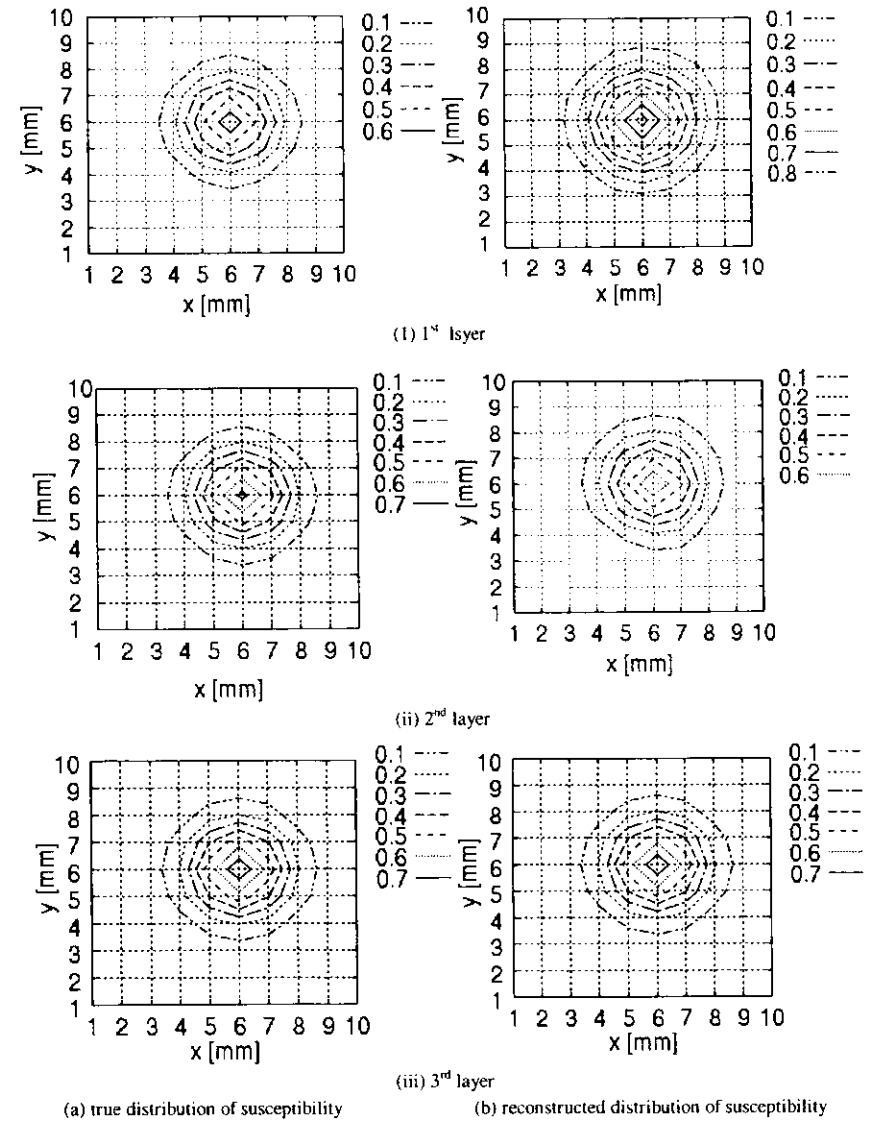


Fig. 10 reconstructed susceptibility

Acknowledgement

We want to thank Dr. Aoto, from JNC, Japan, who generously provided us experimental data for SUS304 specimen. Sincere thanks are also due to Dr. Chen, formerly with JNC, now with JSAEM, for his continuous support for the experimental work and fruitful discussions.

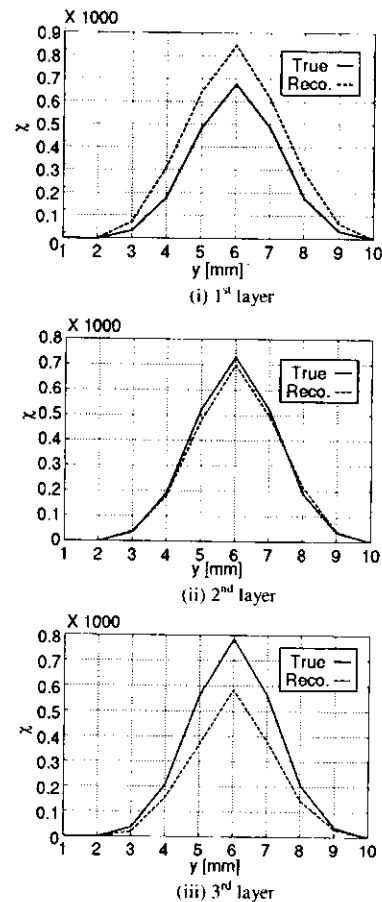


Fig.11 Comparison between true and reconstructed susceptibility

References

- [1] A. Gilanyi, Nondestructive Evaluation of Structural Steels based on Magnetic Property Change, *Ph.D.Thesis*, The University of Tokyo, 1997.
- [2] Z. Chen, K. Aoto and S. Kato, Reconstruction of Magnetic Charges using a Gradient method and Wavelet, Proc. Of 11 SEAD, 15-15 October 1999, Yokohama, Japan, pp. 590-593.
- [3] S. Takaya, G. Preda, K. Demachi, T. Uchimoto and K. Miya, Inverse analysis of magnetization distribution for diagnosis of non-ferromagnetic steel, Proc. of 9th MAGDA Conference, 20-21 March 2000, Australia, pp. 120-123.
- [4] Measurement by VSM, JSAEM internal report, JSAEM-R-9903, 2000, pp.48-54
- [5] Z.Chen and K.Miya, ECT Inversion Using a Knowledge-Based Forward Solver, *J. Nondestr. Eval.*, 17, 3, 1998, pp167-175.
- [6] R.C. Popa and K. Miya, Approximate inverse mapping in ECT, based on aperture shifting and neural network regression, *J. Nondestr. Eval.*, 17, 4, 1998, pp.293-312.

Electromagnetic Damping of Stochastic Barkhausen Discontinuities in Ferromagnets

Valery Vengrinovich

Institute of Applied Physics, Akademicheskaya str. 16, 220072, Minsk, Belarus

Abstract. The problem of Barkhausen noise damping in conductive materials under inspection using a surface probe is considered, the exponential electromagnetic damping with the exponent $\sqrt{2\pi\omega\sigma\mu}/c$ being not assumed a priori. The motivation for new theoretical investigation was reasoned by clear experimental results which have shown, that the real behavior of BN damping is more complex. For this, Barkhausen discontinuities were interpreted as stochastic magnetic dipoles each producing a spherical wave. The simulated function $g(x)$, (where g is the spectral density of the Barkhausen signal and x is the distance between the discontinuity and the coil) compared to the experimental results have shown a good agreement. The new physical model of BN damping can be used for practical applications for estimating the penetration depth of BN testing and for on line solution of inverse problem to estimate surface stresses with depth resolution.

1. Introduction

The magnetic Barkhausen effect (MBE) is commonly used for non destructive evaluation of a ferromagnet's surface layers and can be used to resolve depth information [1]. For this end the problem of attenuation of Barkhausen signals is of great interest. Some investigations made [2-4] start with the assumption that there are plane waves undergoing exponential damping. This point of view has not got still clear experimental evidence. Some experimental observations [5-6] are contradicting as to numerical values of measured attenuation coefficients and to their frequency dependence as well.

First the problem of BN damping was investigated by Deuling and Storm [2] and Heiden and Storm [3]. It was experimentally shown that the magnetic flux in a thin rod surrounded by an inductive coil exponentially decreases as the distance, x , from the discontinuity to the coil increases:

$$F(x) \propto \alpha / 2m_0 \exp(-\alpha x), \quad (1)$$

where α - is a coefficient dependent upon magnetic permeability μ ; m_0 - localized in space increment of magnetic moment caused by discontinuity.

The investigation of BN decay using a surface probe was implemented in [4]. It was assumed that magnetic flux attenuation is exclusively combined with eddy-current damping and that the damping coefficient α is proportional to $\sqrt{2\pi\omega\sigma\mu}$ with ω - spectral frequency of BN and σ - material's conductivity. Neither distance nor the frequency dependence of BN